Investigation of Microgrid Instability Caused by Time Delay

Navid Aghanoori, Mohammad A.S. Masoum, Syed Islam, Steven Nethery
Department of Electrical and Computer Engineering, Centre for Smart Grid and Sustainable Power Systems
Curtin University, WA, Australia
GoldWind Australia Pty Ltd
m.masoum@curtin.edu.au, navid.aghanoori@postgrad.curtin.edu.au, s.islam@curtin.edu.au,
StevenNethery@goldwindaustralia.com

Abstract- **This paper investigates the impact of time delay in the control of a grid-connected microgrid with renewable energy resources. The considered microgrid has a critical load that needs to be powered and protected in the event of grid voltage disturbance while the microgrid maintains connection to the grid. Three case studies are performed considering three different time delays to indicate the advantages of fast communication system in the performance of renewable microgrids. Detailed simulation results illustrate that the proposed communication system using IEC 61850 substation automation standard provides better voltage and current quality to the critical local load with larger phase and gain margins while keeping the microgid connected to main grid.**

1. Introduction

With the inceasing appetite and demand for distributed generation, the role of renewable microgrids has become more significant. Vast numbers of methods and methodologies have been proposed and developed to maximise cost effectiveness, reliability and power quality of microgrids with renewables distrubution genrations (DGs). One of the challenges is how to deal with are the voltage and frequency disturbances. For instance, the control and minimization of power disturbances caused by fluctuations of the natural renewable sources is an ongoing technical challenge [1]. Another chanllege is for the microgids to assist in eliminating the girid disturbance while remaining connected. For instance, Australian wind farm microgrids typically have to maintain their operation if the grid frequency disturbance is either between 47 to 49 or 51 to 52 Hz at least for 2 minutes according to Generator Performance Standard approved by Australian Energy Market Operator (AEMO). This is while the microgrid is expected to trip in the response of frequency above 53 Hz in 100 milliseconds. Combination of these clauses of standard will lead the plants to work in a narrow operation margin for the generation plant [2].
While there are many researches to enhance the performance of renewable microgrids, there is a lack of researche to indicate the consequence of time delays and other real-time factors on the proposed methodologies [3-4]. Ref. [5] presents two methods to limit the current of microgrid in the event of fault ride through from the utility grid to the microgrid. The proposed control methods do not consider the time delay in the real life systems which can entirely affect the capability of the system. This paper continues the research presented in [5] and discusses the practicality of the methods when there is a time delay between the measurement point, the controller and actuators. This paper also proposes a communication model to protect the sensitive load by limiting the fault current while prevents the feeder from tripping.

2. Microgrid Model

Grid-connected microgrids are expected to stay connected to the grid in the event of disturbance from the utility side to avoid voltage and frequency instability due to reduction in power dispatch. For instance, if a large-scale microgrid is disconnected from the grid due to the over frequency or voltage sag conditions, then a large amount of active and reactive power will be automatically removed from the grid that can result in bigger frequency deviations and lower voltage levels. Therefore, it is preferred that the microgrid stays connected to the main grid to help avoiding frequency disturbance and compensate voltage drop by injecting more reactive power at the point of common coupling (PCC) [5].
The overall layout of the microgrid used in this paper based on the model presented in [5] is shown in figure 1. There is a critical load within the microgrid in the downstream side of PCC. This critical load needs to be protected in the event of grid disturbance and voltage sag conditions, which is considered the grid disturbance for this microgrid. As indicated, the microgrid is connected to the grid through a shunt inverter which is a voltage and power regulator while islanded and a synchronizer when connecting to the grid [5]. Additionally, there is a series inverter in the distribution feeder to regulate the current of the feeder when required.

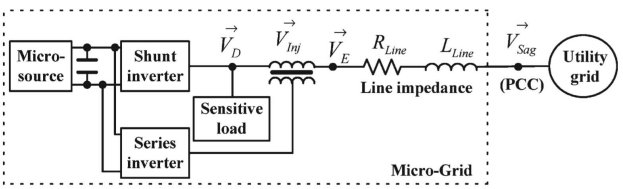

Fig. 1. Single-phase representation of microgrid system under study with specific voltage phasors indicated [5].

2.1. Microgrid Operation Under Voltage Sag

There will be a large current passing through the line impedance when a voltage sag occurs at the PCC. This is purely caused by the voltage difference between point D and PCC. This condition will continue until either the protection system trips on overcurrent fault or voltage sag clears. The voltage difference detected by the sensitive load is:

$$\Delta V = V_D - V_{PCC} \quad (1)$$

To address the aforementioned issue two algorithms are proposed and compared in [5]. The RL feedforward current-limiting algorithm is discussed and compared with the flux-charged-model feedback current limiting algorithm. The second algorithm is proposed as a more robust solution.

2.2. Feedforward Current-Limiting Algorithm [5]

Voltage sag is determined in the PCC; however, if PCC can be located far from the microgrid plant, the voltage sag detection can be implemented at the plant by monitoring the over-current of three phases as the consequence of voltage sag [5]. Once the current exceeds a certain level determined by the system designer then the series inverter applies a large impedance along with series injected voltage of V_{inj} in order to lifts the phasor voltage of point E. This will reduce the voltage difference between grid voltage (V_{sag}) and V_E. The reduction in the voltage difference between grid and point E will consequently reduce the current flowing through the feeder and the critical load. This will also smoothen the recovery of the microgrid when the grid recovers back to the normal operation.

Feedforward current limiting algorithm uses the series inverter to insert virtual impedance and define the voltage reference which is calculated using the line measured current and line impedance. Figure 2 shows how the voltage reference is generated.

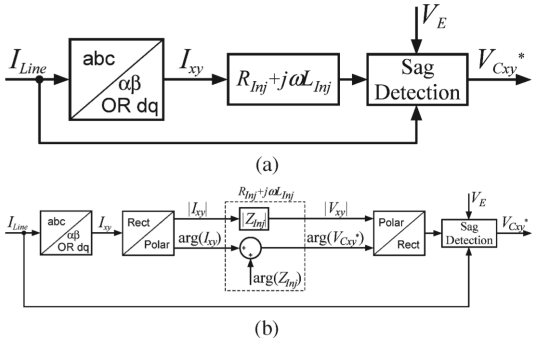

Fig. 2. The RL feedforward current-limiting algorithm [5]; (a) control block diagram, (b) implementation.

Although, this algorithm works in theory it needs more consideration regarding the following aspects:

- Firstly, due to the nature of feedforward concept, the RL algorithm does not have a strong damping performance. This can be promoted by increasing R, which requires rechanneling active power from shunt inverter and a more complex design for selecting proper values of R. To achieve this, an optimal R/L ratio shall be calculated to optimize the injected voltage. This will still end up with undesired power circulation between the series and parallel inverters. It should be noted that the worst-case scenario of the voltage sag must be considered in choosing appropriate R and L values. For the worst case scenario, Ref. [5] considers a voltage drop of in 0.5 p.u. This paper follows the same scenario to make the results comparable with the equivalent simulations without considering real-time time delay.
- Secondly, as can be seen in figure 2 the term S in the transfer function functions as derivative operant. Derivative operant can amplify the noise and to overcome this problem adding a first order pole shall be applied.

Due to the above-mentioned drawbacks of feedforward algorithm, this paper does not explore this algorithm.

3. Flux-Charge-Model Feedback Current-Limiting Algorithm [5]

To avoid the drawbacks of the feedforward RL current-limiting algorithm particularly the power circulation between the inverters, the flux-charge-model feedback current-limiting algorithm introduces an additional closed-loop control algorithm which exclusively injects an inductor (L) in series with the distribution feeder. This algorithm offers to tune the damping without resistive component using controller gains. The flux-charge-model feedback current-limiting algorithm which is based on the extended model presented in [7,8] proposes the flux-charge reference and the flux to be:

$$\Phi_{ref} = -L_0 i_{line} \quad (2)$$

$$\Phi = \int V_C \, dt \quad (3)$$

where V_C and i_{Line} represent the filter-capacitor voltage and the inverter output current of series inverter, respectively.

The flux error is the result of subtracting the flux variable and the reference. The PWM modulator which is represented as $k_{inv} = 2/V_{dc}$ receives the error (Fig. 3). The original model which is shown in figure 3 had the stability problem which has been addressed by adding predictive control component and lead-lag flux regulator. However, adding the abovementioned regulator makes the system sensitive to the parameters [5,7].

Ref. [5] proposes a new scheme using an outer control loop to address the above-mentioned sensitivity issue. The proposed control layout as indicated in figure 4. Figure 5 shows the simplified version of the proposed layout which is used to perform the simulation for this paper. However,

more details of the calculation and algorithm can be found in [5].

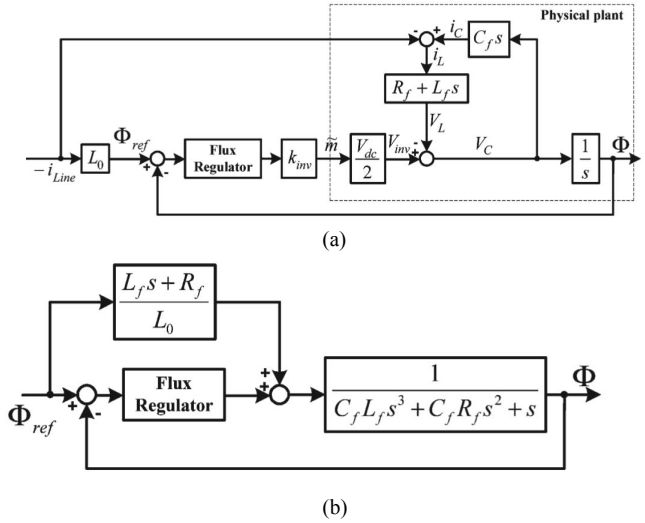

Fig. 3. The flux-charge-model feedback current-limiting algorithm [5]; (a) per-phase control block, (b) simplified per-phase control block representation.

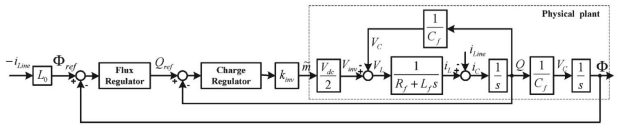

Fig. 4. Control Block representation of flux-charge model algorithm [5].

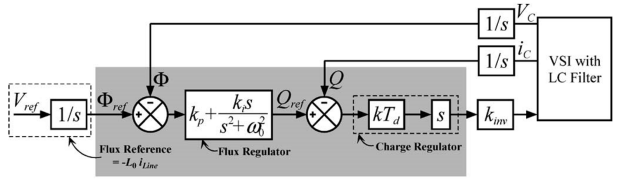

Fig. 5. Modification of flux-charge-model control [5].

4. IEC 61850 Substation Automation and Time Delay

IEC 61850 standard has been published by the International Electrotechnical Commission (IEC) [9]. This substation standard covers the details of communication architecture within the substation. The components that are covered in IEC 61850 include but not limited to circuit breakers, transformers and other protection devices, and is purposed to generate interoperability between the intelligent electronic devices. Interoperability feature can make the communication between different devices and vendors easier and faster. It can also eliminate the consequences and complexity of media converters in the communication system.

4.1. Logical Node and Physical Devices

The intelligent electronic device (IED) is one of the main physical element of the IEC 61850 substation automation standard. IED holds logical nodes (LNs) which are determined in the configuration file of IED. This paper proposes to add the capability of communication into the inverter so that it can be on the IEC 61850 network and have access to the interoperable communication. In the lower level of configuration file, data and data-attribute are determined for each LN. For instance, the status or the position of the circuit breaker can be the data with different data-attitude such as stVal or ctlVal presenting the current value measured by the CT of the feeder. Fig. 6 presents a related example from IEC 61850-7-1 published in 2003 [9]. Unlike the current use of IEDs, this paper proposes to utilize the capability of the IED in the power electronic and decentralized controller devices such as inverters.

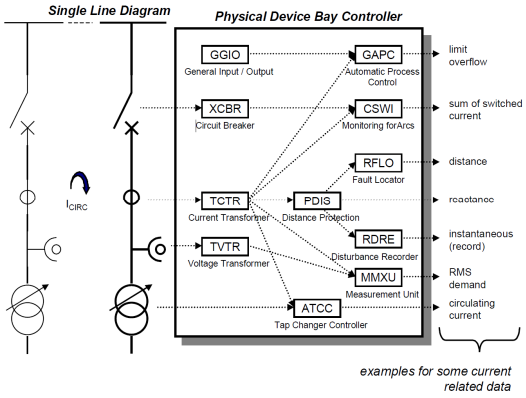

Fig. 6. Control and protection LNs combined in one physical device [9].

The peer-to-peer data exchange model is presented to customize and interface between the measurement and control unit only for renewable application (Fig. 7). It should be noted that the measurement units are already a part of IEC 61850 substation protocol. Therefore, the other end of the control loop must be equipped with this data exchange protocol. The new data exchange model is presented as a part of existing IEC 61850 standard model but it is expected to enhance the data exchange and add interoperability feature between all the renewable measurement and control components. Therefore, by using this model all controllers including decentralized controller in the inverters from different factories can simply communicate without using any media and protocol converters. This will significantly improve the speed of data exchange. Section 5 of this paper presents detailed simulations to investigate the effect of a time delay reduction in the power system.

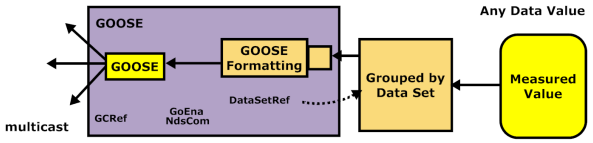

Fig. 7. Peer-to-Peer data exchange model.

The Generic Object-Oriented Substation Event (GOOSE) is chosen and used in figure 7; however, the Sample Value (SV) which can be as fast as GOOSE might be another choice of data type. The difference is that GOOSE needs a trigger point and repeats the same value till the new event based on new trigger points occurs but SV keeps sending the same measured value regardless. The choice between GOOSE and SV will depend on the network traffic management requirement or other aspects of the projects.

4.2. Simulation and Modeling of Time Delay in Flux-Charge-Model Current Limiting Algorithm

The modified flux-charge-model control model of Fig. 5 which is precisely expressed in [5] does not consider the time delays of the real-time system. Figure 8 shows the system block diagram with the added time delay in the control loop. In this paper, the time delay between the measurement unit and controller is considered the main time delay of the control loop.

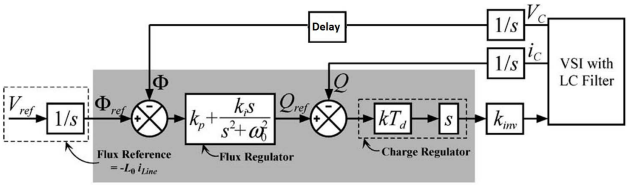

Fig. 8. Flux-charge model control of Fig. 5 with time delay.

5. Simulation Results and Analyses

To demonstrate the benefits of having a fast and interoperable data exchange between the power control and measurement components, this paper simulates and compares the system behavior presented in [5] without and with the addition of time delay between the measurement unit and the controller. The results are compared and analyzed for three different time delays of 1 µs, 1 ms and 5 ms in the event of grid voltage disturbance. To make the simulation results comparable with those presented in Ref. [5], the same voltage drop of 50% is used in the three case studies.

The case studies discuss the voltage and current performance before and after the voltage sag as well as gain and phase margins of the microgrid of Fig. 1 with the specified system parameter of [5]. As aforementioned, the local load is a critical load such that the microgrid needs to stay connected in the event of 0.5 p.u grid voltage disturbance while it shall not exceed 10 amps for more than 200 ms.

5.1. Case A

Figure 9 a and b show the voltage and current of the local load before and after the grid voltage sag, respectively. The time delay for this case is 1 µs. However, this short time delay is not practical and hard to achieve in real networks. As clearly illustrated, the voltage and current signals have a great transient response to the voltage sag. This shows that in practice, there is a margin for the voltage and current to fluctuate in case of any other further disturbance. Figure 10 proves this with indication of relatively large phase and gain margins.

Moreover, the pure sinusoidal voltage and current waves represent less voltage and current harmonics.

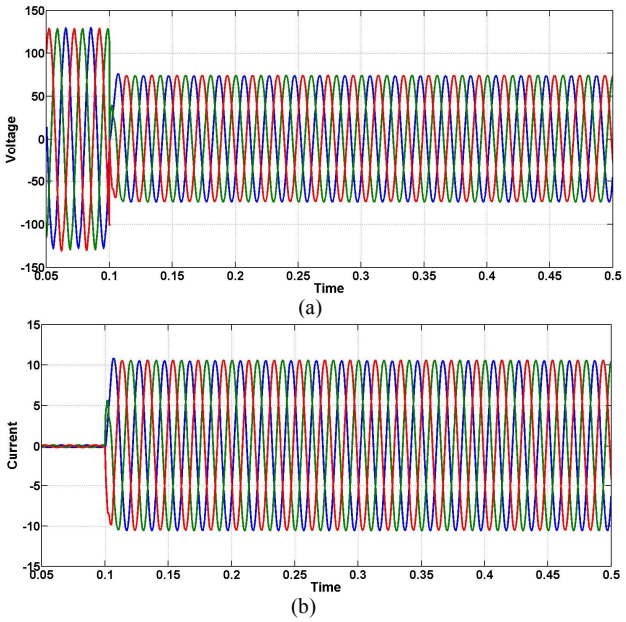

Fig. 9. (a) Critical load voltage (b). Critical load current for time delay = 1 µs.

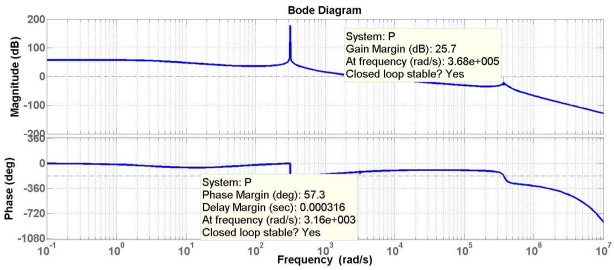

Fig. 10. Bode plot of the microgrid with time delay = 1 µs.

5.2. Case B

Case B investigates the impact of 1 ms time delay in the same microgrid. Figure 11 shows the critical load voltage

and curernt. This time delay has caused a spike in the critical load curernt which exceeded 8 amps. However, it did not exceed the protection setpoint it endagered the system. Therefore, the results are still acceptable from the plant operation point of view.

Likewise the steady state performance of the plant is not as good as Case A with 1 µs delay but it is still within an acceptable range. Note that the voltage and current are not pure sinusoidal indicating the distorted waveforms with some total harmonic distortions (THDs).

Figure 12 also proves a better control of the system through the bode plot which indicates smaller gain and phase margins of the system. According to the results of Figs. 10 and 12 when the time delay has increased from 1 µs to 1 ms, the gain margin and phase margin have been significantly reduced by 72% and 63%, respectively.

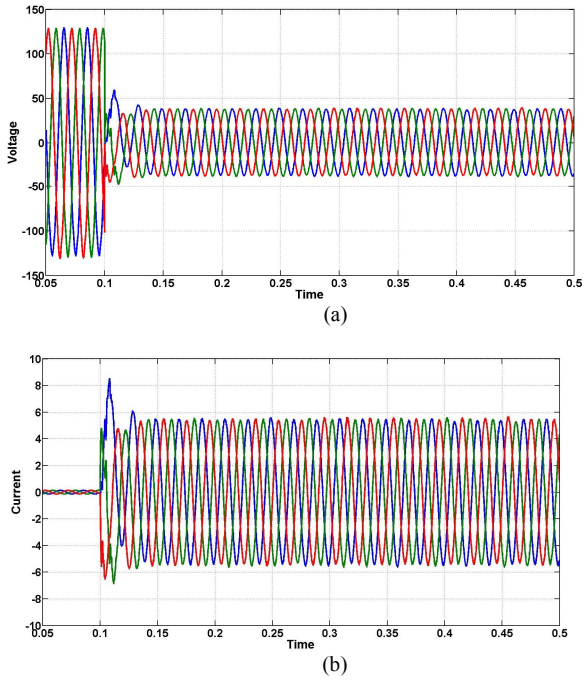

Fig. 11. (a) Critical load voltage (b). critical load current for time delay = 1 ms.

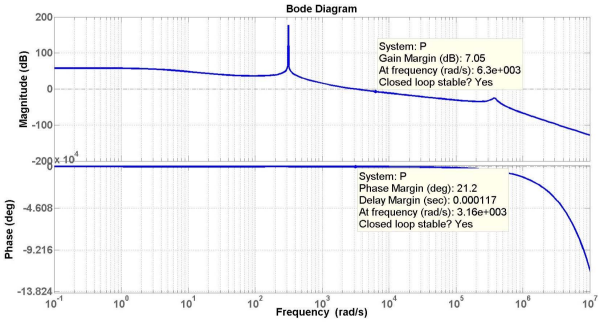

Fig. 12. Bode Plot of the microgrid with time delay = 1 ms.

5.3. Case C

Figure 13 illustrates the voltage and current of critical load before and after the grid voltage disturbance for time delay = 5 ms. The voltage and current seem to be very close to the instability zone. The fluctuations are remarkably significant compared to the system of Case B with time delay of 1 ms. Note that the time delay is not only affecting the transient response to the voltage sag but also it is majorly worsening the system power quality. This is evident from the seriously distorted voltage and current signals with significantly high THD values.

Figure 14 is the bode plot of the same closed loop system when there is 5 ms delay in the communication system of controller and the measurement unit. The gain margin and phase margin have reduced to 5.85 and 17.6. These reductions of 18% and 12% in gain margin and phase margin and the oscillation of the voltage and the current of critical load highlight that system with 5 ms time delay is nearly situated in the instable zone of system operation.

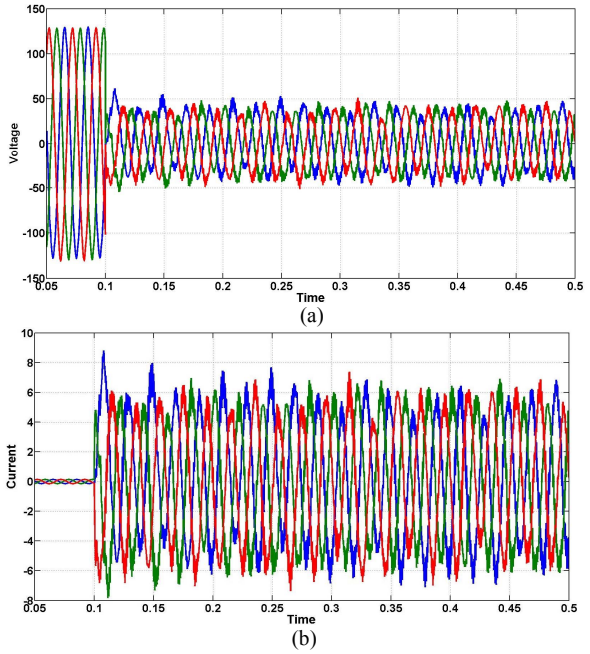

Fig. 13. (a) Critical load voltage (b). Critical load current for time delay = 5 ms.

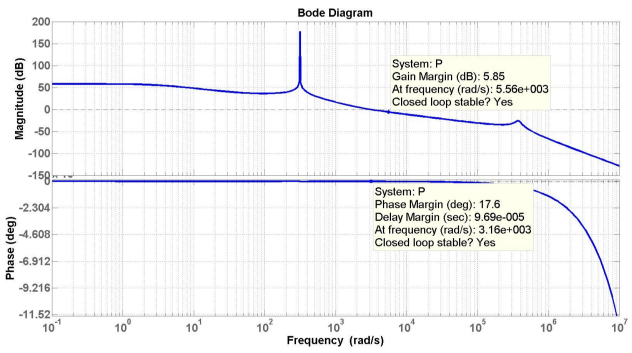

Fig. 14. Bode Plot of the microgrid with time delay = 5 ms.

6. Conclusions

Microgrid has been introduced to power industry as a solution to produce distributed electricity using available local renewable sources. To make the microgrid compliant to the grid codes, they need to stay connected to grid in the event of grid disturbances dictated according to Generator Performance Standard (GPS) and protect their local load. This paper investigates the impact of time delay on the performance of the micogrid.

The micogrid of Ref. [5] with the flux-charge-model feedback current-limiting algorithm is used to protect a critical load in the event of a 0.5 p.u voltage sag at the grid side. Three study cases with time delays of 1 μs, 1 ms and 5 ms are presented to show the voltage and current signals of the critical load before and after grid disturbance as well as the corresponding stability margins. The main conclusions are:

- More fluctuations in the voltage and the current of critical loads are bserved as the time delay is increased. The system with time delay of 1 μs provides the best response of the load voltage and current when the disturbance occurs.
- Time delay has substantial impacts on the gain and phase margins. Increasing the time delay from 1 μs to 1 ms significantly decreases the gain and phase margins by 72% and 63%, respectively. When the time delay is increased to 5 ms, the system operating point is moved closer to the instable zone with further gain and phase margins reductions of 18% and 12%, respectively.
- Time delay has affect the quality of voltage and current signals. However, smaller time delays seem to have less impacts of the THD_v and THD_i.

The abovementioned impacts of time delays in the system stands out the importance of facilitating the microgrids with a fast and interoperable communication system such as IEC 61850. Therefore, this paper proposes the application of GOOSE or SV data types such that the control system components are also able to use the measurement data, which is currently used for protection purposes. This can eliminate the impact of time delay in the system by using customized GOOSE or SV specific for renewable microgrid application while all controllers and measurement units from different vendors can interoperability communicate with minimal time delay.

7. References

[1] S. Choe, Y. K. Son and S. K. Sul, "Control and Analysis of Engine Governor for Improved Stability of DC Microgrid Against Load Disturbance," in *IEEE Journal of Emerging and Selected Topics in Power Electronics*, vol. 4, no. 4, pp. 1247-1258, Dec. 2016.

[2] Australian Energy Market Operator (2016 Sep). Generator Performance Standard. Available at https://www.aemo.com.au/-/media/Files/Doc/0110-0163.

[3] M. S. Manikandan, S. R. Samantaray and I. Kamwa, "Detection and Classification of Power Quality Disturbances Using Sparse Signal Decomposition on Hybrid Dictionaries," in *IEEE Transactions on Instrumentation and Measurement*, vol. 64, no. 1, pp. 27-38, Jan. 2015.

[4] M. Kallamadi and V. Sarkar, "Enhanced real-time power balancing of an AC microgrid through transiently coupled droop control," in *IET Generation, Transmission & Distribution*, vol. 11, no. 8, pp. 1933-1942, 2017.

[5] Y. W. Li, D. M. Vilathgamuwa, and P. C. Loh, "Design, analysis and realtime testing of controllers for multi-bus micro-grid system," *IEEE Trans. Power Electron.,* vol. 19, no. 5, pp. 1195–1204, Sep. 2004.

[6] H. Funato, T. Ishikawa, and K. Kamiyama, "Transient response of three phase variable inductance realized by variable active–passive reactance (VAPAR)," in Proc. *IEEE APEC*, pp. 1281–1286, 2001.

[7] H. Funato, K. Kamiyama, and A. Kawamura, "Transient performance of power circuit including virtual inductance realized by fully digital controlled variable active–passive reactance (VAPAR)," in *Proc. IEEE PESC*, pp. 1195–1200.

[9] IEC for basic communication structure for substation and feeder equipment Principles and models, IEC 61850-7-1, 2003.